Proceedings of the 11th Brazilian Congress of Thermal Sciences and Engineering -- ENCIT 2006
Braz. Soc. of Mechanical Sciences and Engineering -- ABCM, Curitiba, Brazil, Dec. 5-8, 2006

Paper CIT06-0598

EXPERIMENTAL STUDY OF A SOLAR CONCENTRATOR USED IN AN ADSORPTIVE REFRIGERATOR

Rodrigo Ronelli Duarte de Andrade
Laboratório de Energia Solar, Universidade Federal da Paraíba
Cidade Universitária - 58.031-900 João Pessoa-PB, Brazil
rodrigo_ronelli@yahoo.com.br

Moacir Martins Machado
Laboratório de Energia Solar, Universidade Federal da Paraíba
moacir_martins@yahoo.com.br

Antonio Pralon Ferreira Leite
Laboratório de Energia Solar, Universidade Federal da Paraíba
antpralon@yahoo.com.br

Francisco Antônio Belo
Laboratório de Energia Solar, Universidade Federal da Paraíba
belo@ufpb.br

Abstract. In this paper, the different types of solar concentrators used for heating and cooling purposes area described and analyzed. A brief review of the use of solar concentrators is presented, enphasing their application to adsorption refrigeration using the activated carbon-methanol pair. The cooling system we have considered works in an intermittent way without heat recovery. The solar concentrator that is integrated to this system was made in two identical parts, having a semi-cylindrical profile. The concentration ratio is unitary, since the absorbing plate is bifacially irradiated, the total receiver area is equal to the total aperture area. This concentrating collector has a double function: to deviate the radiation to the under side of the absorber during the daytime, and to allow a heat release from the absorber by radiation exchanged with the sky during the nighttime. The infrared net radiant heat flux leaving the absorber has been evaluated by the net-radiation method, based on experimental data obtained for a night period with a predominantly clear sky. The results show that the reflectors deviated about 29% of the energy received by the lower side of the adsorber, and about 32% of the total radiation emitted by the adsorber that reaches the surface openned to the sky and the lateral surfaces of the cavity.

Keywords: radiant heat exchanges, bi-facial collector, solar refrigeration

1. Introdution

The use of the solar energy for several purposes has impeled the development of concentrating collectors of different types and efficiencies. This kind of collector has been applied for water heating, power and cold production.

This paper presents a brief revision about concentrating collectors, standing out the different geometries and their respective applications. A special emphasis is given related to the use of concentrators in adsorption solar refrigeration. In general, besides the required regenerating temperature provided by the solar collector, more is the heat release from it during the nighttime, higher is the coeficient of performance of the cooling system. These two functions can be accomplished by concentrating collectors: to intensify the solar energy hitting the absorber surface and to improve the heat dissipation when the absorbing

Concentrators can be reflectors or refractors, cylindrical or surfaces of revolution, continuous or segmented, imaging or non-imaging concentrators, evacuated or non-evacuated (Duffie and Beckman, 1991). The review we will present next is limited to the concentrator reflectors, continuous and evacuated or non-evacuated.

According to Suzuki and Kobayashi (1995), the most commonly used concentrating collector is a non-imaging concentrator is known as the compound parabolic concentrator (CPC), which was firstly applied to solar energy utilization by Winston and Hinterberger (1975). A two dimensional CPC (2D-CPC) has been proved to be the unique ideal concentrator, as conceived by Welford and Winston (1989).

A CPC with a flat absorber consists of curved segments, which are parts of two parabolas; the CPC reflector profile with a tubular absorber is such that the reflector touches the absorber at the cusp region Duffie *et al*. (1991) (Fig. 1). The most important differences lies in the fact that a fin or tube absorber is illuminated on all sides, requiring only half of the absorber surface, and also that the optical efficiency for the flat receiver will be higher than for the other, since the shape factor of the absorber for the direct radiation is higher.

Tripanagnostopoulos *et. al*. (2000) consider for reducing the absorber thermal losses from CPC collectors three alternative designs of non-evacuated stationary concentrating solar collectors with bifacial absorbers, as shown in Fig. 2.

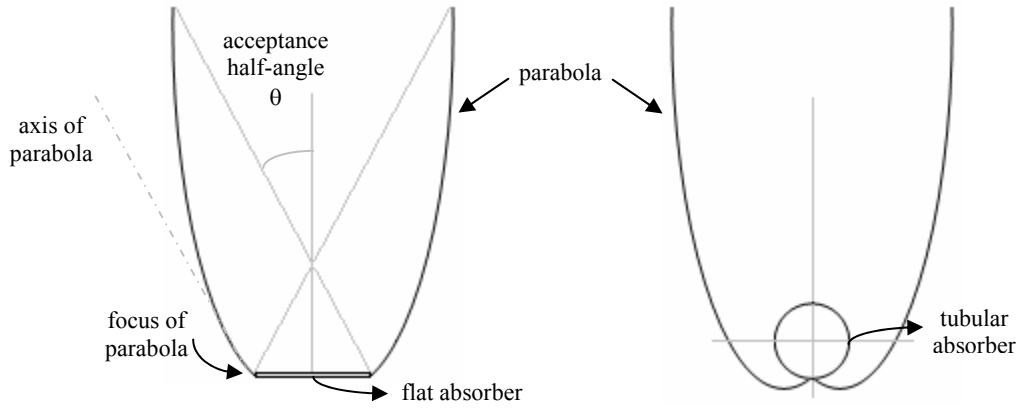

Figure 1. CPC with a flat absorber and a tubular absorber. Adapted from Duffie *et al*. (1991).

The first one (Fig. 2a) is based on an asymmetric mirror and an inverted absorber configurations, in which convection thermal losses are suppressed and higher absorber temperatures can be achieved (Rabl, 1976). The second design (Fig. 2b) thermal losses reduction is obtained by the interposition of a transparent material between the absorber and the cover. Solar collectors with semi-cylindrical reflectors and flat bifacial absorber can be made by covering the absorber with FEP film (Hollands et al., 1991) or with transparent insulation material (Goetzberger et al., 1992). Other technologies include to place transparent baffles into the CPC cavity (Eames and Norton, 1995). The additional transparent material contributes to reduce thermal losses, but the increase of the optical losses must also be taken into account. The third improvement design of CPC (Fig. 2c) considers the use of advanced materials, such as absorbers with coatings of high absorptance and low emittance, mirrors of high reflectance and glazing of high transmittance and heat mirror coatings.

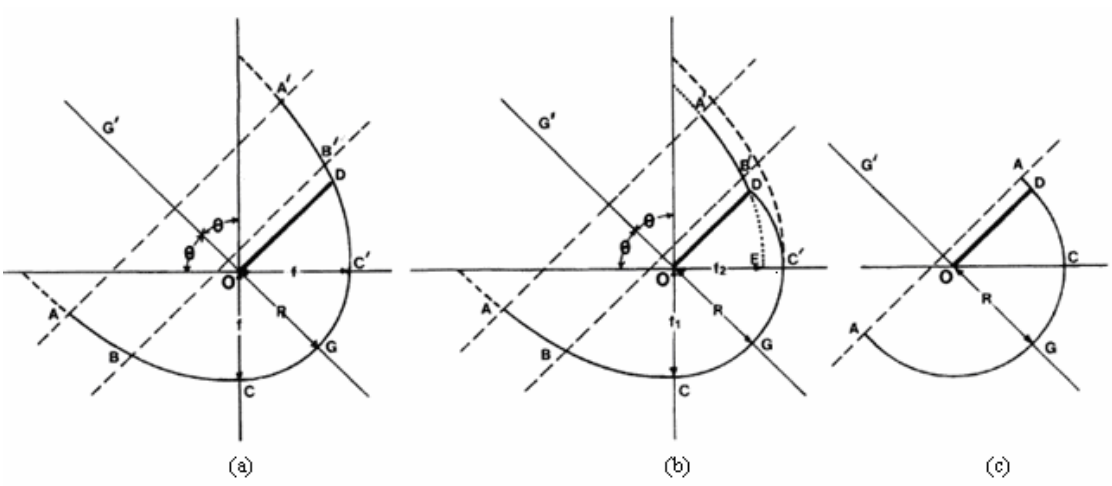

Figure 2. Three alternative designs of non-evacuated stationary concentrating solar collectors with bifacial absorbers (Tripanagnostopoulos *et. al*., 2000)

1.1. Solar concentrator applications.

A potential use of a concentrator is to obtain operating temperatures higher than the water boiling point. In general, the systems having solar concentrators use a fluid to store or to lead the energy received by the absorber. The more commonly used fluid is the water, but ammonia and methanol are also used for solar refrigeration applications.

Besides refrigeration systems (Anyanwu, 2003; Tamainot-Telto and Critoph, 1999; Leite *et al*., 2005), one of the other possible uses for solar concentrators are heating of water (Goetzberger, 1992; Souliotis and Tripanagnostopoulos; 2004; Schmidt and Goetzberger, 1990, Nijegorodov *et al*., 1996) and power generating systems (Lisboa, 2001; Suzuki and Kobayashi, 1995; Brogren *et al*., 2000).

Nijegorodov *et al*. (1996) shows a solar concentrator used for heating and boiling liquids. The concentrator is cylindrical with a linear focus, and the absorber consists of a tube containing water. No glazing was used for either the

concentrator or the absorber tube; in other words, this is a non-evacuated concentrator. Figure 3 shows a cross-section of this concentrator.

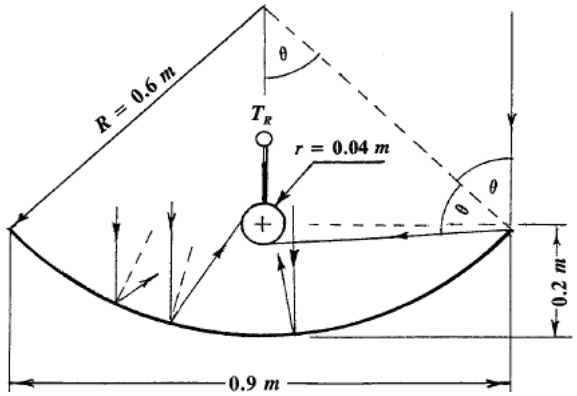

Figure 3. The schematic cross-section of a solar concentrator analyzed for Nijegorodov, N. et al. (1996).

Schmidt and Goetzberger (1990) describe a solar domestic hot water system that uses an integrated collector storage (ICS) with transparent insulation; the same material is used in the system described by Goetzberger *et al*. (1992). In the first case, the system consists of a cylindrical water tank with an integrated collector that is covered with a highly transparent insulation material (TIM). Different designs of this kind of reflector are possible, as shown in Figs. 4a and 4b. In the second case (Fig. 4b), the collector is composed by a flat plate absorber surrounded by transparent insulation material and by two semi-cylindrical mirrors (reflectors).

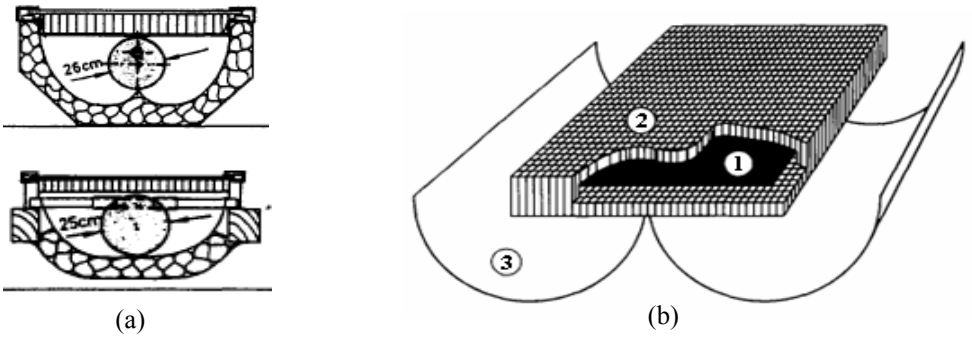

Figure 4. (a) Cross section of ICS prototypes with involutes reflector. (Schmidt and Goetzberger, 1990).
(b) Design of the bifacial-absorber collector. (1) The absorber surrounded by the transparent insulation material (2). The back surface of the absorber is irradiated for two semi-cylindrical mirrors (3) (Goetzberger, A. *et al*., 1992).

Souliotis and Tripanagnostopoulos (2004) show an experimental study on solar water heaters. These solar devices are integrated to collector storage (ICS) systems with single horizontal cylindrical storage tank, which is properly placed in symmetric CPC type reflector trough (Fig. 5).

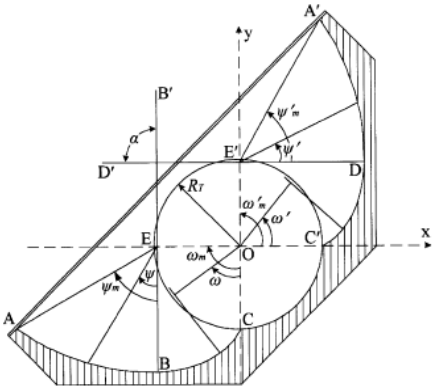

Figure 5. Cross-section of the experimental ICS models (Souliotis and Tripanagnostopoulos, 2004).

Suzuki and Kobayashi (1995) presented a solar electricity generating system, which uses a non-imaging concentrator and economical photovoltaic modules to obtain electricity. Thomas *et al*. (2003) have been developed a study of materials offering a significant cost reduction for solar electricity systems.

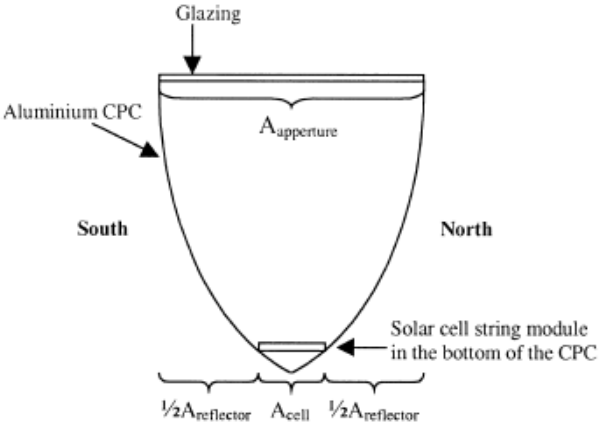

Figure 6. Cross-section of an aluminium compound parabolic concentrator proposed by Brogren, M. et al. (2000).

According to Brogren *et al*. (2000), the cost per energy produced of concentrating hybrid systems is reduced due to the simultaneous heat and electricity production and a reduced photovoltaic cell area. In this system is used a water-cooled photovoltaic-thermal hybrid device with low concentrating aluminum compound parabolic concentrators (Fig.6).

Bezerra (1998) studied the potential of electric energy conversion through thermo-electrical solar, using three classes of concentrators: the tower with heliostats system, the cylindrical-parabolic concentrator and the parabolic plate (Fig. 7).

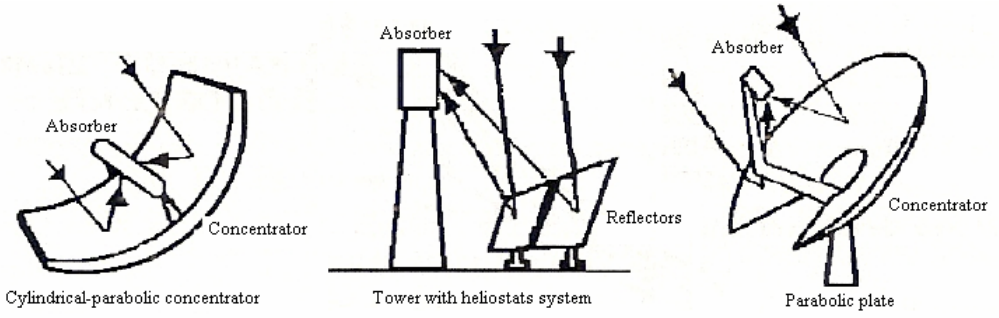

Figure 7. Schemes of three classes of concentrators for power generation. Adapted from Bezerra (1998).

1.2 Solar concentrators applied to solar refrigeration.

The main raison to use concentrators in solar refrigeration is to increase the temperature of the absorbing surface, which is reached by the incidence of the solar radiation also on the lower face of the receiver. Headley *et al*. (1994) (cited in Anyanwu, 2003) built an activated carbon-methanol adsorption refrigerator with a cylindrical-parabolic reflector to concentrate the solar radiation into an adsorbent copper tube at the focal line (Fig. 8a).

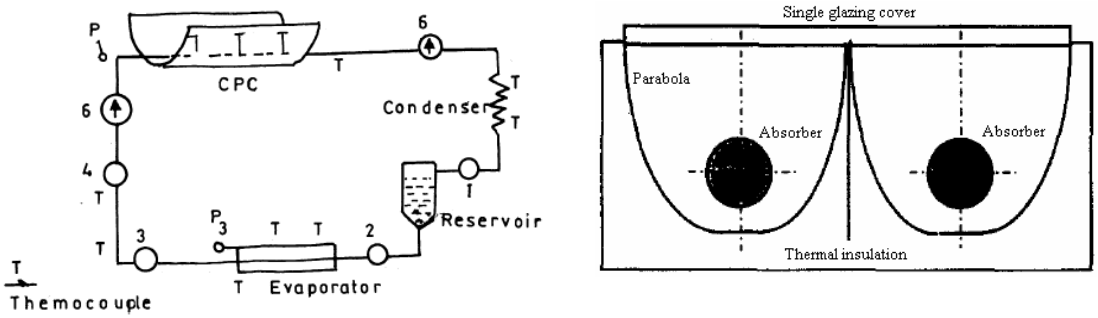

(a) (b)

Figure 8. (a) Scheme of the adsorptive refrigerator with cylindrical-parabolic solar reflector (Anyanwu, 2003); (b) The solar collector of the ammonia-carbon solar refrigerator (Tamainot-Telto and Critoph, 1999).

Tamainot-Telto and Critoph (1999) used two CPC solar collectors with tubular absorbers and a single glazing cover to compose the solar collector of an ammonia-carbon solar refrigerator (Fig. 8b).

Niemann *et al*. (1997) developed and investigated shape concentrators made by segments of parabolas and circles, because of its easiness manufacturing. This kind of collector consists of an evacuated tubular collector with external parabolic circle concentrators (PCC) (Fig. 9). The non-tracking PCC-collector is integrated to an ammonia-carbon adsorption ice maker.

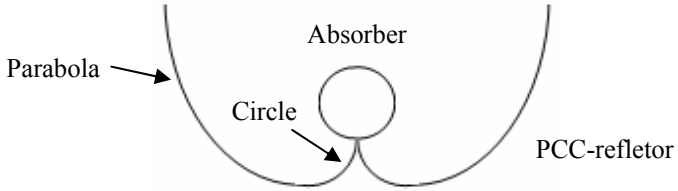

Figure 9. Design of parabolic circle concentrators (PCC). Adapted from Niemann *et al*. (1997).

A semi-cylindrical was used in an adsorptive solar refrigerator that uses the pair activated carbon-methanol. It works in an intermittent cycle, without heat recovery, where the refrigeration effect is produced during night-time and the solar energy is used for regenerating the adsorbent medium (Leite *et al*., 2004; Leite *et al*., 2005a, b). The description and analysis of this concentrator is the main objective of this paper.

2. A solar concentrator integrated to an adsorptive solar refrigerator.

The solar concentrator is part of an adsorber-collector, as shown in Fig. 10. The adsorber consists of a series of steel tubes, placed side by side, making up the radiation absorber plate. The adsorber is filled out by the activated carbon, forming the porous bed.

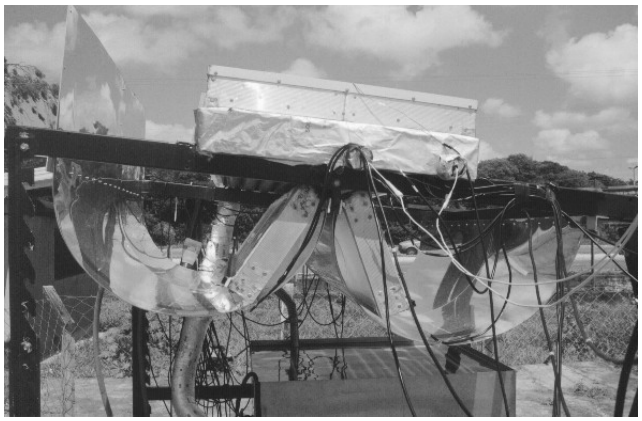

Figure 10. Lateral view of the adsorber-collector.

The adsorber-collector is covered by a capillary structure in polycarbonate that is mounted between two glass plates, the called TIM covers (*transparent insulation material*). Both faces of the adsorber tubes are covered with TIM, and the lower TIM covers are articulated around a central and longitudinal axis, as shown in Fig. 12, while the upper TIM cover is removed by pushing it sideways.

The concentrators are installed bellow the adsorber. They were manufactured in foil of polished aluminum of high reflection index and own semi-cylindrical geometry. The concentrators have a double function: to allow the solar incidence in the lower face of the adsorber, during the regeneration, and to improve its cooling, after the end of desorption, mainly by means of the long wave radiation exchange with the sky. A more detailed description of the adsorber-solar collector can be found in Leite *et al*., 2004.

3. Thermal exchanges in the adsorber.

A detailed analysis about the heat transfers involving the adsorber during the regeneration stage has been made on a recently published (Leite *et al*., 2005b), where several results are carried out based on experimental data. The hourly thermal efficiency was determined by the useful energy method and by the overall heat losses analysis coupled to a graphic model for calculating the optical efficiency. The results were compared to those from a similar adsorptive machine with a flat adsorber covered by a selective surface and by a single glass plate, and they were very close; both daily thermal efficiencies were around 40%.

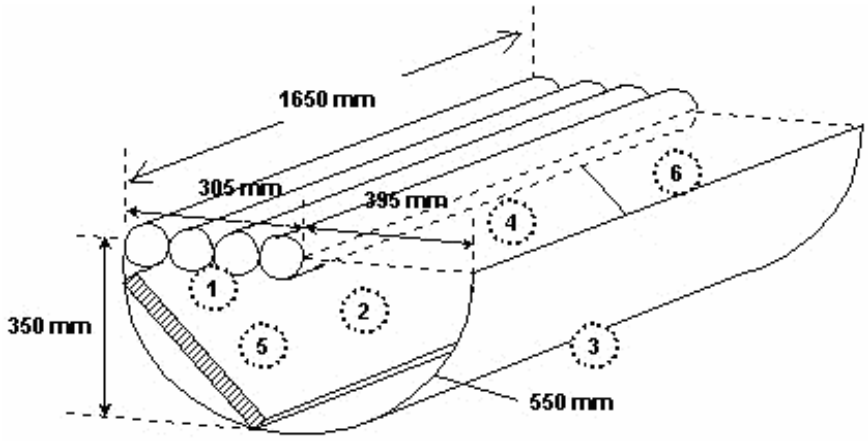

Figure 11. Schematic of the cavity composed by the adsorber and surrounding surfaces.

The thermal exchanges from the adsorber, during the period going from the end of desorption and the end of adsorption, is evaluated to obtain the net radiant fluxes leaving the adsorber by the upper side and by the under side, which is the energy crossing the aperture surface in the zenith direction. Figure 11 shows the cavity considered to analyze the radiant heat interchange between the surfaces surrounding the adsorber, which represents the half of the adsorber. Surface 1 corresponds the tubes (at T_p), surface 2 is the lower TIM cover surface, surface 3 is the reflector, 4 is an opening surface at the sky temperature, and 5 and 6 are opening extremity surfaces at the ambient temperature.

The temperatures of all surfaces were measured, and they are considered uniform, except those concerning the tubes, because in this case, the upper of the adsorber changes radiant heat directly with the sky while the lower face changes radiant heat with the different surfaces composing the cavity.

3.1. Heat transfer equations

Taking into account the symmetry of the physic problem, the energy equation for the half of the adsorber plate can be expressed in a simple form by:

$$m_p Cp_p \frac{\partial T_p}{\partial t} = 2\left\{4\pi D_t L_t \left[h\left(T_p - T_{ac}\right) + h_V\left(T_p - T_{amb}\right)\right] + h_{r,p-sky}\left(T_p - T_{sky}\right) + Q_{r,i}\right\} \tag{1}$$

where m_p is the mass of the tubes, Cp_p is the specific heat, T_p is the temperature, D_t is the diameter, L_t is the length, h is the conductance at the interface tube-adsorbent, T_{ac} is the activated carbon temperature, h_V is the convection coefficient due to wind, T_{amb} is the ambient temperature, $h_{r,p\text{-}sky}$ is an equivalent radiation coefficient and Qr,i is the net radiant heat interchanged with the surfaces composing the cavity. The equivalent sky temperature (T_{sky}) is given by:

$$T_{sky} = \varepsilon_{sky}^{1/4} T_{amb} \tag{2}$$

where ε_{sky} is the apparent emittance of clear sky, given as a function of the dew point temperature (T_{dp}, in ^{o}C), according the following equation given by Berdahl and Martin (1984):

$$\varepsilon_{sky} = 0{,}711 + 0{,}56\left(\frac{T_{dp}}{100}\right) + 0{,}73\left(\frac{T_{dp}}{100}\right)^2 \tag{3}$$

The net radiant flux $Q_{r,i}$ (= Q_1) is determined by the "net-radiation method", based on the Poljak's model (Siegel and Howell, 1992), in which the radiant energy transferred to each surface (Q_j) by convection and conduction is equivalent to the net radiation from this surface, as result of the interchange between all surfaces of the cavity. This energy balance can be written as:

$$Q_j = A_j \frac{\varepsilon_j}{1-\varepsilon_j}\left(\sigma T_j^4 - Q_{o,j}\right) = A_j\left(Q_{o,j} - \sum_{k=1}^{N} F_{j-k}\, Q_{o,k}\right) \tag{4}$$

where A_j is the area of surface j, σ the Stephan-Boltzmann constant, ε_j the emittance of the surface j, N the number of surfaces, F_{j-k} the view factor for the radiant exchange between surfaces j and k, $Q_{o,j}$ the radiant energy leaving surface j, and $Q_{o,k}$ the radiant energy leaving surface k and reaching surface j. All surfaces are considered gray and diffuse, then $\alpha\,(T) = \varepsilon\,(T)$.

For the three-dimensional cavity of Fig. 13, the following equations representing the radiant interchange between the surfaces indicated:

$$\frac{Q_1}{A_1}\left[\frac{1}{\varepsilon_1} - F_{11}\frac{1-\varepsilon_1}{\varepsilon_1}\right] - \frac{Q_2}{A_2}F_{12}\left(\frac{1-\varepsilon_2}{\varepsilon_2}\right) - \frac{Q_3}{A_3}F_{13}\left(\frac{1-\varepsilon_3}{\varepsilon_3}\right) - \frac{Q_4}{A_4}F_{14}\left(\frac{1-\varepsilon_4}{\varepsilon_4}\right) - 2\cdot\frac{Q_5}{A_5}F_{15}\left(\frac{1-\varepsilon_5}{\varepsilon_5}\right) =$$

$$= F_{12}\sigma(T_1^4 - T_2^4) + F_{13}\sigma(T_1^4 - T_3^4) + F_{14}\sigma(T_1^4 - T_4^4) + 2\cdot F_{15}\sigma(T_1^4 - T_5^4) \tag{5}$$

$$-\frac{Q_1}{A_1}F_{21}\left(\frac{1-\varepsilon_1}{\varepsilon_1}\right) + \frac{Q_2}{\varepsilon_2 A_2} - \frac{Q_3}{A_3}F_{23}\left(\frac{1-\varepsilon_3}{\varepsilon_3}\right) - \frac{Q_4}{A_4}F_{24}\left(\frac{1-\varepsilon_4}{\varepsilon_4}\right) - 2\cdot\frac{Q_5}{A_5}F_{25}\left(\frac{1-\varepsilon_5}{\varepsilon_5}\right) =$$

$$= F_{21}\sigma(T_2^4 - T_1^4) + F_{23}\sigma(T_2^4 - T_3^4) + F_{24}\sigma(T_2^4 - T_4^4) + 2\cdot F_{15}\sigma(T_1^4 - T_5^4) \tag{6}$$

$$-\frac{Q_1}{A_1}F_{31}\left(\frac{1-\varepsilon_1}{\varepsilon_1}\right) - \frac{Q_2}{A_2}F_{32}\left(\frac{1-\varepsilon_2}{\varepsilon_2}\right) + \frac{Q_3}{A_3}\left[\frac{1}{\varepsilon_3} - F_{33}\frac{1-\varepsilon_3}{\varepsilon_3}\right] - \frac{Q_4}{A_4}F_{34}\left(\frac{1-\varepsilon_4}{\varepsilon_4}\right) - 2\cdot\frac{Q_5}{A_5}F_{35}\left(\frac{1-\varepsilon_5}{\varepsilon_5}\right) =$$

$$= F_{31}\sigma(T_3^4 - T_1^4) + F_{32}\sigma(T_3^4 - T_2^4) + F_{34}\sigma(T_3^4 - T_4^4) + 2\cdot F_{35}\sigma(T_3^4 - T_5^4) \tag{7}$$

$$-\frac{Q_1}{A_1}F_{41}\left(\frac{1-\varepsilon_1}{\varepsilon_1}\right) - \frac{Q_2}{A_2}F_{42}\left(\frac{1-\varepsilon_2}{\varepsilon_2}\right) - \frac{Q_3}{A_3}F_{43}\left(\frac{1-\varepsilon_3}{\varepsilon_3}\right) + \frac{Q_4}{\varepsilon_4 A_4} - 2\cdot\frac{Q_5}{A_5}F_{45}\left(\frac{1-\varepsilon_5}{\varepsilon_5}\right) =$$

$$= F_{41}\sigma(T_4^4 - T_1^4) + F_{42}\sigma(T_4^4 - T_2^4) + F_{43}\sigma(T_4^4 - T_3^4) + 2\cdot F_{45}\sigma(T_4^4 - T_5^4) \tag{8}$$

$$-\frac{Q_1}{A_1}F_{51}\left(\frac{1-\varepsilon_1}{\varepsilon_1}\right) - \frac{Q_2}{A_2}F_{52}\left(\frac{1-\varepsilon_2}{\varepsilon_2}\right) - \frac{Q_3}{A_3}F_{53}\left(\frac{1-\varepsilon_3}{\varepsilon_3}\right) - \frac{Q_4}{A_4}F_{54}\left(\frac{1-\varepsilon_4}{\varepsilon_4}\right) + 2\cdot\frac{Q_5}{\varepsilon_5 A_5} =$$

$$= F_{51}\sigma(T_5^4 - T_1^4) + F_{52}\sigma(T_5^4 - T_2^4) + F_{53}\sigma(T_5^4 - T_3^4) + F_{54}\sigma(T_5^4 - T_4^4) \tag{9}$$

The areas of the surfaces were obtained from the coordinates of the vertexes of each flat surface (TIM covers, plan of the sky and lateral surfaces) and, also, of the radius of the curved surfaces (reflector and tubes). The value found for each surface was: $A_1 = 0.79$ m^2, $A_2 = 0.67$ m^2, $A_3 = 1.14$ m^2, $A_4 = 0.68$ m^2 e $A_5 = A_6 = 0.21$ m^2.

The assumed emittances were: $\varepsilon_1 = 0.95$, $\varepsilon_2 = 0.88$ e $\varepsilon_3 = 0.20$, and the apparent emittance of the sky (ε_4) was calculated by Eq. (3) at each hour, ranging from 0.86 to 0.89. Along the lateral surfaces, it was considered the emittance effective average of the air around any surface, given for Stein and Reynolds (1999), $\varepsilon_5 = \varepsilon_6 = 0.82$.

A computational program was developed to calculate the view factors. From the definition given by Siegel and Howell (1992), the program found nine form factors and then, knowing that $F_{2\text{-}2} = F_{4\text{-}4} = F_{5\text{-}5} = F_{6\text{-}6} = 0$, the other factors could be determined utilizing the following equations:

$$A_i\,F_{i-j} = A_j\,F_{j-i} \tag{10}$$

$$\sum_{j=1}^{N} F_{i-j} = 1 \tag{11}$$

The three-dimensional view factors are showing in Table (1).

Table 1. Three-dimensional view factors for the radiant exchange.

Surface	F_{1-j}	F_{2-j}	F_{3-j}	F_{4-j}	F_{5-j}	F_{6-j}
1 - Tubes	0.280	0.328	0.182	0.048	0.268	0.268
2 - TIM covers	0.277	0	0.179	0.255	0.172	0.172
3 - Reflectors	0.263	0.306	0.085	0.650	0.463	0.463
4 - Sky	0.041	0.260	0.387	0	0.078	0.078
5 - Lateral surface 1	0.070	0.053	0.084	0.024	0	0.019
6 - Lateral surface 2	0.070	0.053	0.084	0.024	0.019	0
Total	**1**	**1**	**1**	**1**	**1**	**1**

4. Results and discussion

Leite *et al*. (2005b) have made a bi-dimensional analysis of the cavity. In this study, the equations system represented by Eqs. (5) to (9) was solved by using the inverse matrix method, from experimental measurements of the surfaces temperatures and meteorological parameters, such as the ambient temperature, wind velocity and humidity, carried out during a typical clear sky day.

Tables 2, 3 and 4 shows the results for temperature data obtained for October-December period. Each one represents a specified cycle and the considered period (15 p.m. to 4 a.m.) was defined from experimental data, according to Leite *et al*. (2005a, b). The calculations of the hourly net radiant heat ($Q_{r,i}$) by each surface of the cavity indicated in Fig. 11, i.e., the period between the end of the regeneration and the end of the adsorption. The indicated times represent a centered hour.

Table 2. Hourly net radiant heat fluxes by each surface of the cavity in October.

Time	$Q_{r,1}$ (W)	$Q_{r,2}$ (W)	$Q_{r,3}$ (W)	$Q_{r,4}$ (W)	$Q_{r,5}$ (W)	$Q_{r,6}$ (W)
15h00	-5.1	-52.6	-2.6	50.3	5.0	5.0
16h00	-11.9	-25.9	-6.0	46.6	-1.4	-1.4
17h00	-8.2	-23.0	-6.9	44.2	-3.1	-3.1
18h00	-5.0	-12.5	-4.7	27.6	-2.8	-2.8
19h00	2.1	4.6	2.2	-8.3	-0.4	-0.4
20h00	-39.1	14.7	2.3	15.5	3.3	3.3
21h00	-26.5	8.7	1.6	12.7	1.8	1.8
22h00	-10.9	16.3	5.1	-13.6	1.5	1.5
23h00	-18.1	0.9	-1.5	18.5	0.1	0.1
00h00	-13.4	-4.3	-3.3	22.9	-0.9	-0.9
01h00	-11.8	-6.3	-4.7	24.8	-1.0	-1.0
02h00	-9.2	-6.2	-3.8	22.0	-1.4	-1.4
03h00	-8.0	-11.0	-5.3	28.4	-2.1	-2.1
04h00	-8.0	-8.7	-3.8	24.4	-2.0	-2.0

Table 3. Hourly net radiant heat fluxes by each surface of the cavity in November.

Time	$Q_{r,1}$ (W)	$Q_{r,2}$ (W)	$Q_{r,3}$ (W)	$Q_{r,4}$ (W)	$Q_{r,5}$ (W)	$Q_{r,6}$ (W)
15h00	-42.4	-2.1	-1.5	37.8	4.2	4.2
16h00	-19.4	-14.7	-6.8	45.1	-2.1	-2.1
17h00	-11.6	-13.4	-7.9	41.1	-4.1	-4.1
18h00	-6.0	-7.8	-5.2	25.6	-3.3	-3.3
19h00	2.1	7.2	1.5	-9.9	-0.5	-0.5
20h00	-11.9	4.7	-0.7	8.9	-0.5	-0.5
21h00	-6.5	2.0	-1.2	7.9	-1.1	-1.1

22h00	0.2	10.7	3.5	-16.3	0.9	0.9
23h00	-5.9	-4.1	-3.1	16.8	-1.9	-1.9
00h00	-8.7	-4.9	-4.0	22.3	-2.3	-2.3
01h00	-7.8	-6.5	-4.6	24.3	-2.7	-2.7
02h00	-8.1	-3.5	-4.4	20.9	-2.5	-2.5
03h00	-8.2	-8.7	-5.8	29.0	-3.1	-3.1
04h00	-7.4	-7.5	-5.0	25.6	-2.9	-2.9

Table 4. Hourly net radiant heat fluxes by each surface of the cavity in December.

Time	$Q_{r,1}$ **(W)**	$Q_{r,2}$ **(W)**	$Q_{r,3}$ **(W)**	$Q_{r,4}$ **(W)**	$Q_{r,5}$ **(W)**	$Q_{r,6}$ **(W)**
15h00	-18.6	-8.4	-9.0	34.9	0.5	0.5
16h00	-19.9	-14.4	-8.4	47.2	-2.2	-2.2
17h00	-16.9	-14.6	-7.9	45.8	-3.2	-3.2
18h00	-7.8	-8.9	-5.3	28.2	-3.1	-3.1
19h00	0.2	6.0	1.5	-7.4	-0.1	-0.1
20h00	-12.5	0.8	-0.7	12.9	-0.2	-0.2
21h00	-8.3	2.5	-1.8	9.4	-0.9	-0.9
22h00	-0.3	10.7	3.3	-15.6	0.9	0.9
23h00	-8.3	-2.0	-3.2	17.5	-2.0	-2.0
00h00	-8.2	-4.7	-4.1	22.2	-2.6	-2.6
01h00	-8.8	-5.8	-4.7	24.8	-2.7	-2.7
02h00	-7.9	-7.5	-1.6	21.3	-2.1	-2.1
03h00	-7.8	-8.6	-3.9	25.8	-2.8	-2.8
04h00	-7.2	-5.0	-2.6	20.6	-2.9	-2.9

Based on average values obtained over the whole calculation period, the radiation emitted by the tubes (surface 1) that attains the TIM cover (surface 2) represents 27.7%, while that that reaches directly the reflector (surface 3) is about 26.3%. Only 4.1% passes directly through the aperture (surface 4), 14% traverses directly the surfaces 5 and 6, and about 27.9% from the total emitted by surface 1 reaches itself. The radiant energy that passes through the apertures (surface 1, 5 and 6) represents 32% of the total emitted by the tubes. Figure (12) show hourly emitted and received radiant energy by each surface of the cavity for the data of October.

The total heat released from the upper side of the adsorber by radiative exchanges with the sky corresponds to 76% of the total heat dissipated from it. Concerning only the losses by radiation, the upper side is responsible for 89%, while the side lower is responsible for 11% of the total.

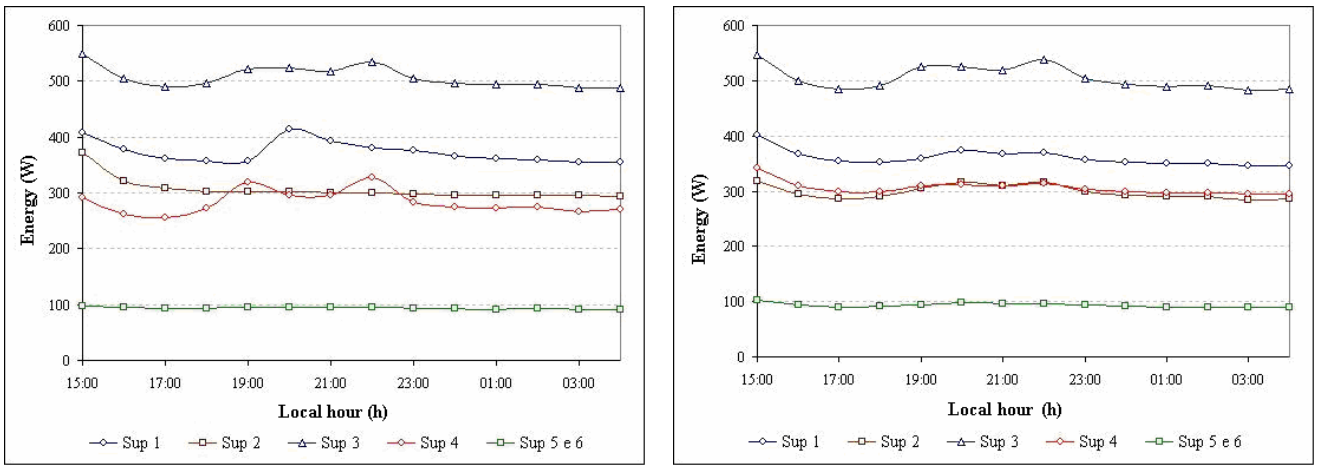

(a) (b)

Figure 12. (a) Hourly emitted energy and (b) received by each surface of the cavity in October.

6. Conclusion

A brief revision about the different formats and uses of solar concentrators was presented. A special emphasis was given to the use of a concentrator in an adsorptive solar refrigerator that uses the activated carbon-methanol pair, where the concentrator is integrated to the adsorber component. The results from calculations have shown that the concentrator deviates about 29% of the energy received from the under side of the adsorber and about 32% of the radiant energy emitted to the sky and to the lateral surfaces.

5. References

Anyanwu, E. E., 2003, "Rewiew of Solid Adsorption Solar Refrigerator I: An overview of the Refrigeration Cycle", Energy Conversion & Management, Vol.44, pp. 301-312.

Berdahl, P. and Martin, M., 1984, "Emissivity of Clear Skies", Solar Energy, Vol.32, N° 5, pp. 663-664.

Bezerra, A. M., 1998, "Aplicações Térmicas da Energia Solar", Ed. Universitária UFPB, J. Pessoa, Brazil, 242 p.

Brogren, M., Nostell, P. and Karlsson, B., 2000, "Optical efficiency of a PV-Thermal Hybrid CPC Module for High Latitudes", Solar Energy, Vol.69 (Suppl.), N° 1-6, pp. 173-185.

Duffie, J. A. and Beckman, W. A., 1991, "Solar Engineering of Thermal Processes", 2nd Ed. John Wiley, New York, U.S.A.

Eames, P. C., and Norton, B., 1995, "Thermal and Optical Consequences of the Introduction of Baffles into Compound Parabolic Concentrating Solar Energy Collector Cavities", Solar Energy, Vol.55, pp. 139-150.

Goetzberger, A., Dengler, J., Rommel, M. Götischf, J. and Wittwer, V., 1992, "A New Transparently Insulated, Bifacially Irradiated Solar Flat-Plate Collector", Solar Energy, Vol.49, N° 5, pp. 403-411.

Hollands, K. G. T. Brunger, A. P. and Morrison, I. D., 1991, "Evaluating Improvement to a Low-concentrating-ratio, Non-evacuated, Non-imaging Solar Collector", In: Procceding of Int. Conf. Solar World Congress Biennial Meeting of ISES, Vol.2, Part II, pp. 1860-1865, Denver, USA.

Leite, A.P.F., Grilo M.B., Andrade R.R.D. and Belo F.A., 2004, "Dimensioning, Thermal Analysis and Experimental Heat Loss Coefficients of an Adsorptive Solar Icemaker", Renewable Energy, Vol.29, pp. 1643-1663.

Leite, A.P.F., Grilo M.B., Andrade R.R.D., Belo F.A. and Meunier, F., 2005a, "Experimental Evaluation of a Multi-Tubular Adsorber operating with Activated Carbon-Methanol", Adsorption - Journal of Int. Adsorption Society, Vol. 11, pp. 543-548.

Leite, A.P.F., Grilo M.B., Andrade R.R.D., Belo F.A. and Meunier, F., 2005b, "Thermal Exchanges in a Bi-facially Irradiated Collector Integrated to an Adsorptive Solar Refrigerator", In Proc. COBEM 2005 18th International Congress of Mechanical Engineering, 6-11 November, Ouro Preto, MG, Brazil.

Lisboa, A. H., 2001, "Determinação do Potencial de Conversão de Energia Elétrica através de Termelétrica Solar – Metodologia e Demonstração de Caso para Belo Horizonte", Proceedings of XVI Seminário Nacional de Produção e Transmissão de Energia Elétrica, Vol.1, Campinas , São Paulo, Brazil.

Niemann, M., Kreuzburg, J., Schreitmüller, K. R. and Leppers, L., 1997, "Solar process heat generation using an ETC coletor field with external parabolic circle concentrador (PCC) to operate on adsortion refrigeration system". Solar Energy, v.59, n. 1-3, p. 67-73.

Nijegorodov, N., Jain, P. K. and Devan, k. R. S., 1996, "A Graphical Method of Measuring the Performance Characteristics of Solar Collectors", Renewable Energy, Vol.7, N° 1, pp. 23-31.

Rabl, A., 1976, "Comparison of Solar Concentrators", Solar Energy, Vol.18, pp. 93-111.

Schmidt, C. and Goetzberger, A., 1990, "Single-Tube Integrated Collector Storage Systems with Transparent Insulation and Involucre Reflector", Solar Energy, Vol.45, N° 2, pp. 92-100.

Siegel, R. and Howell, J.R., 1992, "Thermal Radiation Heat Transfer", 3rd Ed. Taylor & Francis Pub., Washington, USA.

Souliotis, M. and Tripanagnostopoulos, Y., 2004, "Experimental Study of CPC type ICS Solar Systems", Solar Energy, Vol.76, pp. 389-408.

Stein, B.. Reynolds, J., 1999, "Mechanical and Electrical Equipment for Buildings", 9th Ed., Ed. John Wiley & Sons, New York, EUA, 1999.

Suzuki, A. and Kobayashi, S., 1995, "Yearly Distributed Insolation Model and Optimum Design of a Two Dimensional Compound Parabolic Concentrator", Solar Energy, Vol.54, N° 5, pp. 327-331.

Tamainot-Telto, Z. and Critoph, R. E., 1999, "Solar Sorption Refrigerador Using a CPC Collector", Renewable Energy, Vol.16, pp. 735-738.

Tripanagnostopoulos, Y., Yianoulis, P., Papaefthimiou, S. and Zafeiratos, S., 2000, "CPC Solar Collectors with Flat Bifacial Absorbers", Solar Energy, Vol.69, N° 3, pp. 191-203.

6. Copyright Notice